Available online at www.sciencedirect.com

ScienceDirect

journal homepage: www.elsevier.com/locate/he

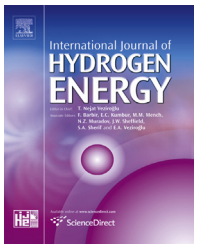

Performance evaluation of an alkaline fuel cell/thermoelectric generator hybrid system

Puqing Yang [a], *Ying Zhu* [a], *Pei Zhang* [a], *Houcheng Zhang* [a,*], *Ziyang Hu* [a], *Jinjie Zhang* [b]

[a] *Department of Microelectronic Science and Engineering, Ningbo University, Ningbo 315211, China*
[b] *School of Marine Science, Ningbo University, Ningbo 315211, China*

ARTICLE INFO

Article history:
Received 31 March 2014
Received in revised form
23 May 2014
Accepted 26 May 2014
Available online 20 June 2014

Keywords:
Alkaline fuel cell
Thermoelectric generator
Hybrid system
Irreversible loss
Performance evaluation

ABSTRACT

A hybrid system consisting of an AFC (Alkaline Fuel Cell), a TEG (Thermoelectric Generator) and a regenerator is put forward, where the AFC converts the chemical energy in the hydrogen into electrical energy and thermal energy, and the released thermal energy is subsequently converted into electrical energy through the bottoming TEG. The main irreversible losses in each element of the hybrid system are characterized, and numerical expressions for the efficiency and power output of the AFC, TEG and hybrid system are respectively derived. The fundamental relation between the operating current density of the AFC and the dimensionless current of the TEG is obtained, from which the region of the operating current density of the AFC that the TEG exerts its function is determined. By employing such a hybrid system, the equivalent maximum power density of the AFC can be increased by up to 23%. The effects of the operating current density, operating temperature, heat conductivity, and integrated parameter on the performance of the hybrid system are revealed. The results obtained in the present paper will provide some theoretical guidance for the performance improvement of the AFC.

Introduction

Fuel cells have the potential to lower the environmental burden of meeting domestic energy needs, particularly greenhouse gas emissions and primary energy consumption [1]. Low-temperature fuel cells, can be widely used in the fields such as power generation, transportation, and portable power, which constitute an important element in pollution-free energy conversion [2,3]. Because the predicted low cost and high durability in PEMFCs remain problematic, a resurgence of interest in the AFC (Alkaline Fuel Cell) has been attracted in recent years [4–9]. AFCs can be manufactured from relatively standard materials and do not need precious metals or energy intensive sintering, and their balance of plant is less complicated than that of other type fuel cell systems.

However, the major drawback of an AFC is its comparative low power density, which becomes a critical factor that restricts the widely commercialization of AFCs [10]. The maximum power density obtained from AFCs has undergone many advances in recent years not only due to the progresses in catalysts and electrode materials but also due to the optimized operating conditions and fuel cell design [11]. As an

* *Corresponding author*. Tel.: +86 574 87600770; fax: +86 574 87600744.
E-mail address: zhanghoucheng@nbu.edu.cn (H. Zhang).
http://dx.doi.org/10.1016/j.ijhydene.2014.05.166
0360-3199/

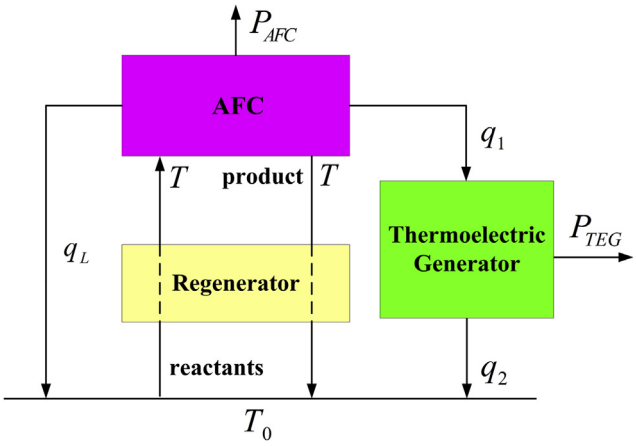

Fig. 1 – The schematic diagram of an AFC-TEG hybrid system.

alternative approach, the equivalent maximum power density of low-temperature fuel cells can be also effectively elevated by employing cogeneration systems to recover the waste heat produced in the fuel cell for other applications [12–18]. Zhang et al. [12] established a new three-heat-reservoir cycle based AFC hybrid system and found that the waste heat produced in the AFC can be readily used in such a system. Hwang et al. [15,16] developed a heat recovery unit and implemented it in a PEM fuel cell cogeneration system to produce electricity and hot water simultaneously. Ishizawa et al. [17] presented a PAFC (phosphoric acid fuel cell) energy system for telecommunication cogeneration systems, where the PAFCs are applied to provide electrical power to telecommunication equipment and the waste heat is used by absorption refrigerators to cool the telecommunication rooms. Zhao et al. [18] carried out the parametric studies on a hybrid power system by integrating a PEM fuel cell stack with an organic Rankine cycle to recover the waste heat from PEM fuel cell stack.

TEG (Thermoelectric Generator) can convert thermal energy into electricity due to the Seebeck effect, which is regarded as one of the potential candidates for renewable energy conversion [19,20]. Besides being environmentally friendly, TEGs have many other advantages such as being highly reliable, adapting to different kinds of heat reservoirs and having no moving parts. Therefore, TEGs have received more and more attention in scientific community especially in the aspect of low-level waste heat recovery [21]. Obviously, the waste heat generated in the AFC can be further converted into electricity through a bottoming TEG and thus the equivalent maximum power density of AFC can be effectively enhanced.

In the present paper, a hybrid system mainly composed of an AFC, a TEG and a regenerator is put forward to increase the equivalent maximum power density of the AFC. The performance of the hybrid system is evaluated by taking the main irreversible losses in each element of the system into account. The availability of the hybrid system will be validated and the effects of some operating conditions and designing parameters on the performance of the hybrid system will be revealed. Some possible problems that should be aware in the practical operation of the hybrid system are posed.

An AFC-TEG hybrid system

The hybrid system established here consists of an AFC, a TEG and a regenerator, where the TEG is closely attached to the AFC, as schematically shown in Fig. 1. The AFC acts as the high-temperature heat reservoir of the TEG which generates an additional power generation, and the regenerator is applied to preheat the incoming fuel and oxidant with the comparative high-temperature exhaust product from the AFC. By using such a hybrid system, the heat produced in the AFC can be effectively harvested, and consequently, the equivalent maximum power density of the AFC can be improved. Below, each component in the hybrid system will be analyzed, and then the performance characteristics of the global system will be synthetically investigated.

The AFC

The AFC directly converts the chemical energy of the incoming hydrogen into the electrical and thermal energies, it is mainly composed of an anode and a cathode with KOH solution as an electrolyte sandwiched between the two electrodes. The AFC is operated by introducing hydrogen as fuel and oxygen as oxidant to the anode and cathode, respectively. At the anode, hydrogen reacts with hydroxyl ions available in the KOH solution into water and releases electrons to the external electric circuit. At the cathode, oxygen reacts with water into hydroxyl ions with the help of the reaching electrons. The overall electrochemical reaction is

$$H_2 + \frac{1}{2}O_2 \rightarrow H_2O + \text{Heat} + \text{Electricity}. \quad (1)$$

As previously described in Ref. [22], some irreversible losses in the AFC are inevitably when the above electrochemical reaction is occurred, and these irreversible losses can be characterized in terms of activation overpotential (V_{act}), concentration overpotential (V_{con}) and ohmic overpotential (V_{ohm}). By considering these three overpotentials, the power output and efficiency of an AFC can be, respectively, expressed as [22]

$$P_{AFC} = jA(E - V_{act} - V_{ohm} - V_{con}), \quad (2)$$

and

$$\eta_{AFC} = \frac{P_{AFC}}{-\Delta\dot{H}} = \frac{n_e F}{-\Delta h}(E - V_{act} - V_{con} - V_{ohm}), \quad (3)$$

where $E = [-\Delta g_f^0 + (T - T_0)\Delta s^0 + RT\ln(p_{H_2}\sqrt{p_{O_2}}/p_{H_2O})]/n_eF$ is the equilibrium potential; Δg_f^0 is the standard molar Gibbs free energy change at reference condition ($T_0 = 298$ K, $p_0 = 1$ atm), Δs^0 is the standard molar entropy change, both of them can be founded in Ref. [22]; R is the universal gas constant; T is the operating temperature of the AFC; n_e is the number of mole electrons transferred per mole hydrogen; F is the Faraday's constant; p_{H_2}, p_{O_2} and p_{H_2O} are respectively the partial pressures of H_2, O_2, and H_2O, and the water produced is assumed to be in liquid phase, such that $p_{H_2O} = 1$ atm; j is the electric current density; A is the polar plate area of the AFC; $(-\Delta\dot{H}) = -jA\Delta h/(n_eF)$ is the total energy released per unit

time, Δh is the molar enthalpy change at temperature T; $V_{act} = RT\ln(j/j_0)/(\beta n_e F)$, β is the transfer coefficient, $j_0 = c_1 \exp(-c_2/T)$ is the exchange current density, c_1 and c_2 are two constants; $V_{con} = RT\ln[j_L/(j_L - j)]/(\beta n_e F)$, j_L is the limiting electric current density; $V_{ohm} = jt_{ele}/\kappa$, t_{ele} is the thickness of the aqueous KOH electrolyte, κ is the specific conductivity of the aqueous KOH solution electrolyte which is related to the operating temperature and KOH solution concentration, and there exists an optimum electrolyte concentration for different operating temperature at which the ohmic overpotential achieves its minimum [22].

The regenerator

The regenerator in the hybrid system acts as a counter-flow heat exchanger, which heats the reactants from the ambient temperature to the operating temperature of AFC by using the heat contained in the comparative high-temperature product. If the efficiency of the regenerator, ε, equals to 100%, the regenerator is ideal and an additional heat input is unnecessary. Owing to the existence of thermal resistance, some regenerative losses are inevitable and some additional heat from the AFC should be transferred to compensate the losses. Assuming the rate of the regenerative losses is directly proportional to the temperature difference between the AFC and the environment, the regenerative losses is given by Refs. [23,24]

$$q_{re} = K_{re}A_{re}(1-\varepsilon)(T - T_0), \tag{4}$$

where K_{re} and A_{re} are, respectively, the heat-transfer coefficient and heat-transfer area of the regenerator.

The TEG

The TEG in the hybrid system is composed of many n- and p-type semiconductor legs that are connected electrically in series by metal strips and thermally in parallel, as show in Fig. 2. The thermoelectric generating elements are assumed to be insulated, both electrically and thermally, from their surroundings, except at the junction-reservoir contact. The current is assumed to flow along the arms of the generator. When the TEG operates stably, the boundary conditions are determined by $T_1(0) = T_2(0) = \ldots T_i(0) = \ldots = T_n(0) = T$ and $T_1(L) = T_2(L) = \ldots T_i(L) = \ldots = T_n(L) = T_0$, where L is the arm length of the generator. For simplification, the temperature of the hot junction, T_1, is assumed to be equal to that of the AFC, T, and the temperature of the cold junction, T_2, is assumed to be equal to that of the environment, T_0. Thus, the heat conductions of a multi-couple TEG between the AFC and the environment can be, respectively, expressed as follows [25,26]

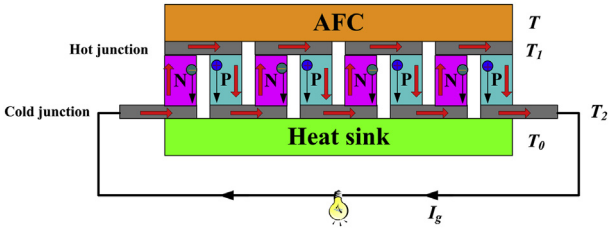

Fig. 2 – The schematic diagram of a multi-couple TEG.

$$q_1 = \alpha I_g T - 0.5I_g^2 R + K(T - T_0), \tag{5}$$

and

$$q_2 = \alpha I_g T_0 + 0.5I_g^2 R + K(T - T_0), \tag{6}$$

where $\alpha = (\alpha_p + \alpha_n)m$ is the total Seebeck coefficient, the subscripts "p" and "n" stand for p- and n-type semiconductors, m is the number of TEG couples; $R = (\rho_p l_p/S_p + \rho_n l_n/S_n)m$ is the total electrical resistance, ρ is the electrical resistivity, l is the length of the semiconductor arms, S is the cross-sectional areas of semiconductor arms; $K = (\kappa_p S_p/l_p + \kappa_n S_n/l_n)m$ is the total thermal conductance, κ is the thermally conductivity of the semiconductor materials; I_g is the operating electrical current of a multi-couple TEG, I_g^2R represents the Joule heat resulted from the electrical resistance in the TEG; and $K(T - T_0)$ denotes the heat leak due to the temperature difference between the hot and cold junctions. It has been proved by Holman [27] that when the relation between the structure parameters l_p/S_p and l_n/S_n, i.e., $l_n/S_n = (l_n/S_n)\sqrt{\kappa_n\rho_p/\kappa_p\rho_n}$, is satisfied, the geometric configuration of the TEG is in the optimum form and the electrical resistance and thermal conductance of a multi-couple TEG can be, respectively, expressed as

$$R = m\left(\rho_p + \sqrt{\frac{\rho_p\rho_n\kappa_n}{\kappa_p}}\right)\left(\frac{l_p}{S_p}\right), \tag{7}$$

$$K = m\left(\kappa_p + \sqrt{\frac{\kappa_p\kappa_n\rho_n}{\rho_p}}\right)\left(\frac{S_p}{l_p}\right). \tag{8}$$

Using Eqs. (5) and (6), the power output and efficiency of the TEG can be, respectively, expressed as [28]

$$P_{TEG} = q_1 - q_2 = K(T - T_0)J - KJ^2/Z, \tag{9}$$

and

$$\eta_{TEG} = \frac{P_{TEG}}{q_1} = \frac{Z(T - T_0)J - J^2}{Z(T - T_0) + ZTJ - J^2/2}, \tag{10}$$

where $J = \alpha I_g/K$ and $Z = \alpha^2/(KR)$ are, respectively, the dimensionless current and the figure of merit of the TEG. As described by Eqs. (9) and (10), both the power output and the efficiency are larger than zero when some heat are transferred from the AFC to the TEG, i.e., $P_{TEG} > 0$ and $\eta_{TEG} > 0$, and thus the dimensionless current of the TEG is located in the following region

$$0 < J < Z(T - T_0). \tag{11}$$

The efficiency and power output of the hybrid system

As illustrated in Fig. 1, the total thermal energy released in the AFC is divided into three parts. Besides the part used to replenish the regenerative losses, another part is transferred to the TEG for electricity generation and the rest part is directly leaked into the environment via convective and/or

conductive heat transfer. The part leaked into the environment can be expressed as [29,30]

$$q_L = \alpha_L A_L (T - T_0), \tag{12}$$

where α_L is the convective and/or conductive heat-leak coefficient and A_L is the effective heat-transfer area. According to the first law thermodynamics, the part of the heat transferred to the TEG is given by

$$\begin{aligned} q_1 &= -\Delta\dot{H} - P_{AFC} - q_{re} - q_L \\ &= -\frac{A\Delta h}{n_e F}\left[(1-\eta_{AFC})j - \frac{n_e F c_3 (T - T_0)}{-\Delta h}\right], \end{aligned} \tag{13}$$

where $c_3 = [K_{re}A_{re}(1-\varepsilon) + \alpha_L A_L]/A$ is an integrated parameter which is related to the heat transfer irreversibilities, effective heat-transfer areas and polar plate area of the AFC.

By considering the heat leak between the hot and cold junctions, the TEG in the hybrid system begins to exert its function only when the following condition is satisfied:

$$-\Delta\dot{H} - P_{AFC} > q_{re} + q_L + K(T - T_0). \tag{14}$$

Substituting Eqs. (2), (4) and (12) into Eq. (13), Eq. (14) can be further explicitly rewritten as

$$j > j_C = \left[\frac{n_e F}{-\Delta h(1-\eta_{AFC})}\right][c_3(T - T_0) + K(T - T_0)/A], \tag{15}$$

where j_C is the critical operating current density of the AFC from which the TEG in the hybrid system starts to work. When $j > j_C$, the fundamental relation between the operating current density of the AFC, j, and the dimensionless current of the TEG, J, is determined by the following equation:

$$J^2 - 2ZTJ - 2Z(T - T_0) + \frac{2ZA}{K}\left[\frac{-\Delta h}{n_e F}(1-\eta_{AFC})j - c_3(T - T_0)\right] = 0. \tag{16}$$

Combining Eqs. (11) and (16), one may easily determine the maximum operating current density of the AFC, j_M, from which the TEG in the hybrid system stops working. Thus, the TEG in the hybrid system is not operated in the entire operating current density region of AFC but works in the following region

$$j_C < j < j_M. \tag{17}$$

Table 1 – Parameters used in the modeling [22,31–33].

Parameter	Value
Faraday constant, F (C mol^{-1})	96,485
Number of electrons, n_e	2
Universal gas constant, R (J mol^{-1} K^{-1})	8.314
Fuel composition, P_{H_2}; $P^{fuel}_{H_2O}$ (atm)	0.97; 0.03 [22]
Partial pressure of O_2, P_{O_2} (atm)	1
Partial pressure of product H_2O, P_{H_2O} (atm)	1
Constant, c_1 (A m^{-2})	174,512 [31]
Constant, c_2 (K)	5485 [31]
Constant, c_3 (W m^{-2} K^{-1})	1.0 [31]
Transfer coefficient, β	0.1668 [31]
Limiting current density, j_L (A m^{-2})	2000 [31]
Thickness of the electrolyte, t_{ele} (m)	0.001 [32]
Effective area of the AFC, A (m^2)	9.0×10^{-4}
Temperature of the AFC, T (K)	353
Temperature of environment, T_0 (K)	298.15
Heat conductivity, K (W K^{-1} m^{-1})	1.5×10^{-2} [33]

Based on Eqs. (2), (3), (9), (10) and (16), the numerical expressions of the power output and efficiency of the hybrid system can be, respectively, expressed as

$$P = P_{AFC} + P_{TEG} = VjA + KT_0[(T/T_0 - 1)J - J^2/(ZT_0)], \tag{18}$$

and

$$\eta = \frac{P_{AFC} + P_{TEG}}{-\Delta\dot{H}} = \eta_{AFC} + \frac{n_e F K T_0[(T/T_0 - 1)J - J^2/(ZT_0)]}{-jA\Delta h}. \tag{19}$$

It is worthwhile to mention that j and J in Eqs. (18) and (19) are not independent of each other, and the relationship between j and J is given by Eq. (16).

Results and discussion

As shown by Eqs. (18) and (19), the performance of the TEG-based AFC hybrid system depends on a set of thermodynamic and electrochemical parameters such as the operating temperature, electric current density, electrolyte thickness, electrolyte concentration, electrical resistance and thermal conductance of the TEG, figure of merit of the thermoelectric materials, structure parameters of the TEG, and so on. To quantitatively investigate the influence of these parameters on the performance of the hybrid system, numerical calculations are carried out based on the parameters summarized in Table 1 [22,31–33], and these parameters are kept constants unless specifically mentioned.

The efficiency and the power density of the hybrid system varying with the operating current density of the AFC are clearly shown in Figs. 3 and 4, where $P^* = P/A$ is the power density, P^*_{max} is the maximum power density, and j_P is the operating current density corresponding to P^*_{max}. It is observed that the power density of the hybrid system first increases and then decreases as the operating current density is increased, while the efficiency first rapidly decreases then slightly increases and finally decreases as the operating current density increases. The efficiency slightly increases in the region of $j_C < j < j_M$ because the increase in the efficiency contributed by the TEG is larger than the decrease in efficiency caused by the AFC. For the typical parameters given in Table 1, numerical calculation shows that the power density of the hybrid system attains its maximum P^*_{max}, 204.48 W/m^2, when the operating current density $j = 1051$ A/m^2, while the power density of the AFC achieves its maximum $P^*_{AFC,max}$, 166.20 W/m^2, when the operating current $j = 934$ A/m^2, and the maximum power density of the hybrid system is about 23% larger than that of the sole AFC. Meanwhile, the efficiencies of the hybrid system and AFC corresponding to their maximum power densities are, respectively, 13.1% and 11.9%, and the efficiency of the hybrid system is about 10.1% larger than that of the sole AFC. It clearly shows that the performance of the AFC can be effectively enhanced by coupling TEGs to the AFCs for further converting the produced waste heat into electricity, and the increase in the power density is more obvious than that in the efficiency.

It is also seen from Figs. 3 and 4 that the efficiency and power density of the hybrid system are affected by the

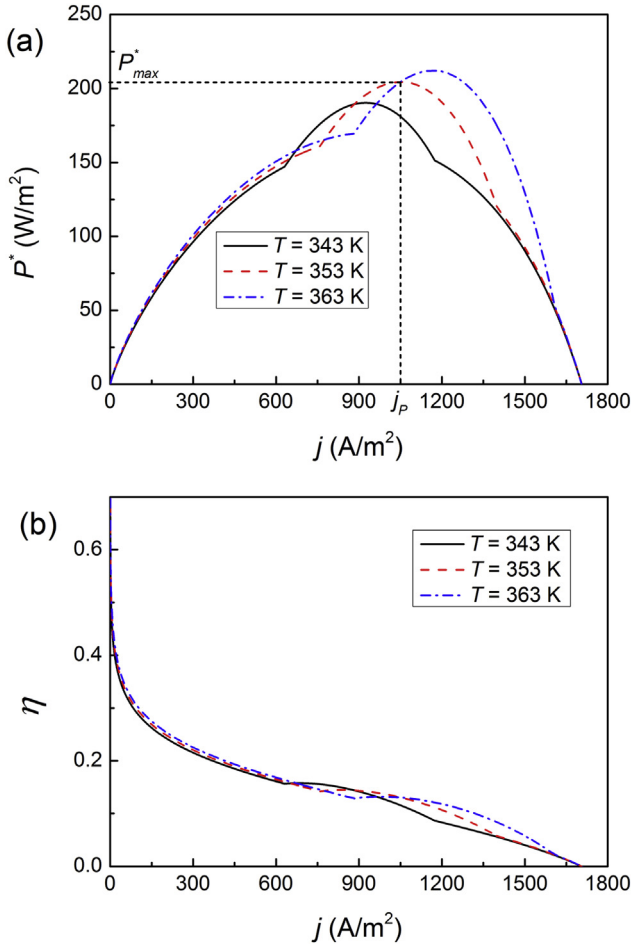

Fig. 3 – The effects of operating temperature *T* on the (a) power density, and (b) efficiency of the hybrid system, where P^*_{max} is the maximum power density, and j_P is the operating current density corresponding to P^*_{max}.

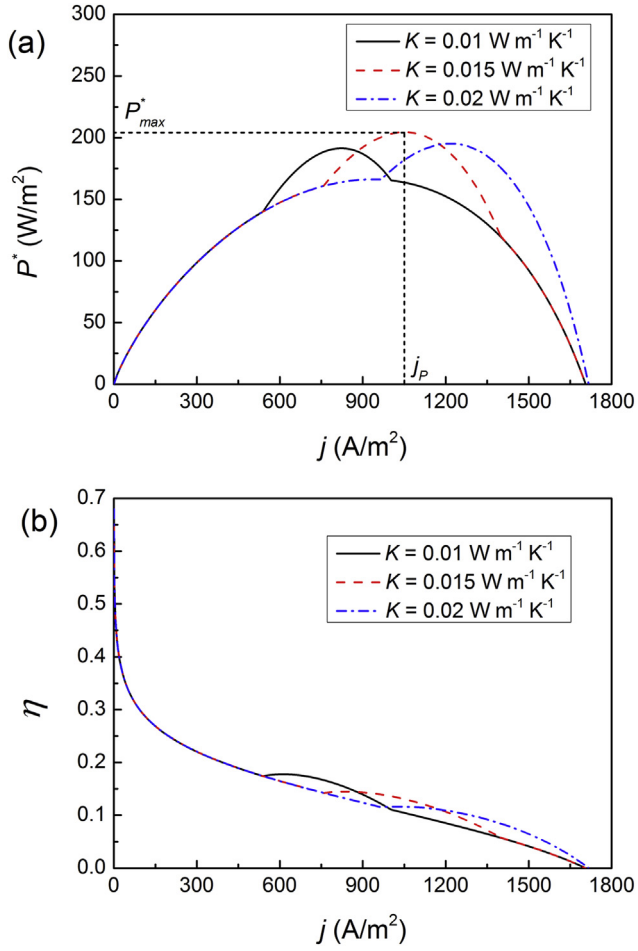

Fig. 4 – The effects of heat conductivity *K* on the (a) power density, and (b) efficiency of the hybrid system.

operating temperature *T*, and the thermal conductance of the TEG *K*. It is seen that the effects of operating temperature and thermal conductance on the efficiency of the hybrid system are not as significant as that on the power density. When $j < j_C$ or $j > j_M$, the efficiency and power density are increased with increasing operating temperature *T*, while both of them are not sensitive to the change of thermal conductance *K*. The values of j_C, j_M and j_P shift to larger ones as the operating temperature *T* or thermal conductance *K* is increased, and j_P is usually located between j_C and j_M. The operating current

Table 2 – The values of j_C, j_M, j_P and P^*_{max} for different operating temperature *T* and thermal conductance *K*, where $c_3 = 1.0\ W\ m^{-2}\ K^{-1}$.

T (K)	K (W K^{-1} m^{-1})	j_C (A/m^2)	j_M (A/m^2)	$\Delta j = j_M - j_C$ (A/m^2)	j_P (A/m^2)	P^*_{max} (W/m^2)
343	0.01	448	832	384	717	170.85
	0.015	631	1173	542	925	190.36
	0.02	807	1483	676	1083	193.09
	0.025	976	1747	771	1202	183.50
353	0.01	540	1003	463	823	191.39
	0.015	759	1400	641	1051	204.48
	0.02	967	1734	767	1216	195.25
	0.025	1164	1948	784	1334	169.70
363	0.01	630	1168	538	924	209.15
	0.015	882	1606	724	1166	212.16
	0.02	1119	1914	795	1331	186.46
	0.025	1342	1997	655	934	170.00

density interval Δj ($=j_M - j_C$) that the TEG exerts its function increases as the operating temperature T or the thermal conductance K is increased. It is also seen from Fig. 4 (a) that there is an optimum value of the thermal conductance K at which the maximum power density can be expected. For the typical parameters given in Table 1, the optimum value of K is found to be between 0.01 W K^{-1} m^{-1} and 0.02 W K^{-1} m^{-1}. Based on numerical calculation, more detailed values of j_C, j_M, Δj, j_P and P^*_{max} under different operating temperature T and thermal conductance K are listed in Table 2. It is interesting to note from Table 2 that there is a counter-example, i.e., the case with $T = 363$ K and $K = 0.025$ W K^{-1} m^{-1}, that j_P is smaller than j_C and Δj is smaller than that with smaller operating temperature or that with smaller thermal conductance. For this case, the maximum power density of the hybrid system is the same as that of the sole AFC, and thereby, increasing the equivalent maximum power density of the AFC by coupling a multi-couple TEG to the AFC is in vain. In practical operation, engineers should carefully choose the proper pairs of operating temperature of AFC and thermal conductance of TEG to ensure that the AFC-TEG cogeneration system is effective.

The influence of the integrated parameter, c_3, on the performance of the hybrid system is clearly shown in Fig. 5. It is observed from Fig. 5 that this influence is only occurred in the region of $j_C < j < j_M$, the power density and efficiency decrease with the increasing parameter c_3, while the current densities j_C, j_M, and j_P increase as the parameter c_3 is increased. When the heat-leak from the AFC to the environment and the regenerative losses in the regenerator are negligible, i.e., $c_3 = 0$, the fundamental relation between the operating current density of the AFC and the dimensionless current of the TEG can be reduced from Eq. (16) to

$$J^2 - 2ZTJ - 2Z(T - T_0) + \frac{2ZA}{K}\left[\frac{-\Delta h}{n_e F}(1 - \eta_{AFC})j\right] = 0. \quad (20)$$

For this case, the curves of the power density and efficiency varying with the operating current density are shown by the black solid line in Fig. 5.

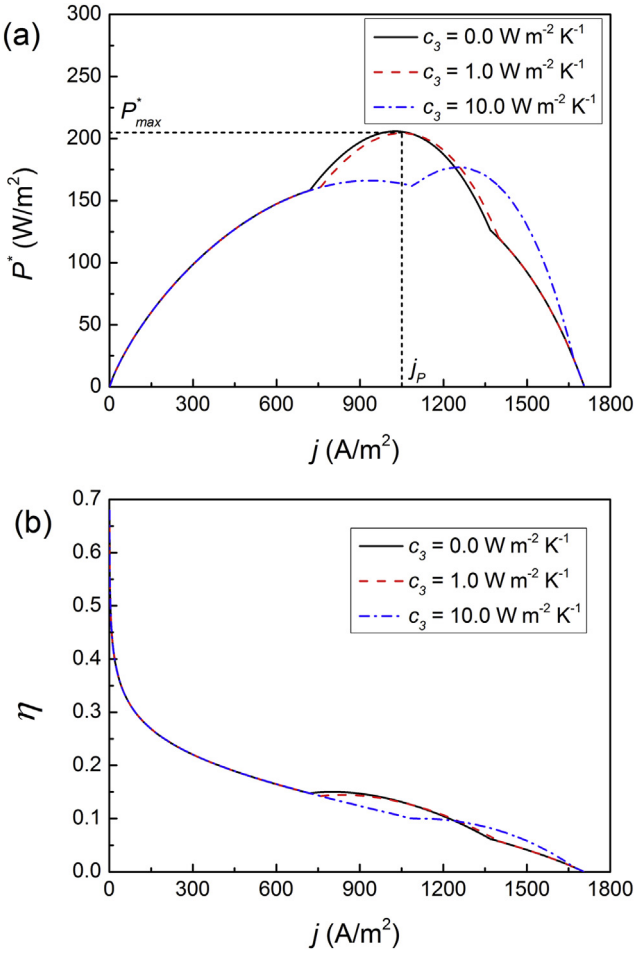

Fig. 5 – The effects of integrated parameter c_3 on the (a) power density, and (b) efficiency of the hybrid system.

Conclusions

An AFC-TEG hybrid system composed of an AFC, a multi-couple TEG and a regenerator is established to effectively recover the waste heat released in the AFC. By considering the main thermodynamic-electrochemical irreversibilities in the system, the analytical expressions of the performance parameters for the hybrid system are derived, and from which the general performance characteristics are revealed. The operating current density interval that the TEG exerts its function is determined. It is found that the performance of the AFC can be effectively improved by coupling a TEG to the AFC for additional power generation, and the improvement in the efficiency is less significant as that of the power density. The influences of the operating temperature and operating current density of the AFC, thermal conductance of the TEG and integrated parameter c_3 on the performance of the hybrid system are revealed. The results obtained in the paper may offer some theoretical guidance for the performance improvement of an AFC through cogeneration systems.

Acknowledgments

This work has been supported by the National Natural Science Foundation of China (Grant Nos. 11347173, 11304170), the Natural Science Foundation of Zhejiang Province of China (Grant No. LQ14E06002), the Natural Science Foundation of Ningbo City (Grant Nos. 2013A610139, 2013A610033), the Foundation of Zhejiang Educational Commission (Grant Nos. Y201326937, Y201326905, Y201430419), the Zhejiang Open Foundation of the Most Important Subjects (Grant No. xkzw108), the Scientific Research Project of Ningbo University (Grant No. XYL14005), and the K. C. Wong Magna Fund in Ningbo University.

REFERENCES

[1] Acres GJK. Recent advances in fuel cell technology and its applications. J Power Sources 2001;100:60–6.
[2] Srinivasan S, Mosdale R, Stevens P, Yang C. Fuel cells: reaching the era of clean and efficient power generation in

twenty-first century. Annu Rev Energy Environ 1999;24:281–328.
[3] Oliveira VB, Simoes M, Melo LF, Pinto AMFR. Overview on the development of microbial fuel cells. Biochem Eng J 2013;73:53–64.
[4] Gülzow E. Alkaline fuel cells: a critical view. J Power Sources 1996;61:99–104.
[5] Burchardt T, Gouerec P, Sanchez-Cortezon E, Karichev Z, Miners JH. Alkaline fuel cells: contemporary advancement and limitations. Fuel 2002;81:2151–5.
[6] Bidault F, Brett DJL, Middleton PH, Abson N, Brandon NP. A new application for nickel foam in alkaline fuel cells. Int J Hydrogen Energy 2009;34:6799–808.
[7] Bidault F, Brett DJL, Middleton PH, Abson N, Brandon NP. An improved cathode for alkaline fuel cells. Int J Hydrogen Energy 2010;35:1783–8.
[8] Gouérec P, Poletto L, Denizot J, Sanchez-Cortezon E, Miners JH. The evolution of the performance of alkaline fuel cells with circulating electrolyte. J Power Sources 2004;129:193–204.
[9] McLean GF, Niet T, Prince-Richard S, Djilali N. An assessment of alkaline fuel cell technology. Int J Hydrogen Energy 2002;27:507–26.
[10] Kimble MC, White RE. A mathematical model of a hydrogen/oxygen alkaline fuel cell. J Electrochem Soc 1991;138:3370–82.
[11] Verhaert I, Verhelst S, Janssen G, Mulder G, De Paepe M. Water management in an alkaline fuel cell. Int J Hydrogen Energy 2011;36:11011–24.
[12] Zhang X, Chen J. Maximum equivalent power output and performance optimization analysis of an alkaline fuel cell/heat-driven cycle hybrid system. J Power Sources 2011;196:10088–93.
[13] Barelli L, Bidini G, Gallorini F, Ottaviano A. An energetic-exergetic analysis of a residential CHP system based on PEM fuel cell. Appl Energy 2011;88:4334–42.
[14] Kordesch K, Gsellmann J, Cifrain M, Voss S, Hacker V, Aronson RR, et al. Intermittent use of a low-cost alkaline fuel cell-hybrid system for electric vehicles. J Power Sources 1999;80:190–7.
[15] Hwang JJ, Zou ML, Chang WR, Su A, Weng FB, Wu W. Implementation of a heat recovery unit in a proton exchange membrane fuel cell system. Int J Hydrogen Energy 2010;35:8644–53.
[16] Hwang JJ, Zou ML. Development of a proton exchange membrane fuel cell cogeneration system. J Power Sources 2010;195:2579–85.
[17] Ishizawa M, Okada S, Yamashita T. Highly efficient heat recovery system for phosphoric acid fuel cells for cooling telecommunication equipment. J Power Sources 2000;86:294–7.
[18] Zhao P, Wang J, Gao L, Dai Y. Parametric analysis of a hybrid power system using organic Rankine cycle to recover waste heat from proton exchange membrane fuel cell. Int J Hydrogen Energy 2012;37:3382–91.
[19] Sahin AZ, Yilbas BS. Thermodynamic irreversibility and performance characteristics of thermoelectric power generator. Energy 2013;55:899–904.
[20] Ali H, Sahin AZ, Yilbas BS. Thermodynamic analysis of a thermoelectric power generator in relation to geometric configuration device pins. Energ Convers Manage 2014;78:634–40.
[21] Gou X, Yang S, Xiao H, Ou Q. A dynamic model for thermoelectric generator applied in waste heat recovery. Energy 2013;52:201–9.
[22] Zhang H, Lin G, Chen J. The performance analysis and multi-objective optimization of a typical alkaline fuel cell. Energy 2011;36:4327–32.
[23] Zhang H, Lin G, Chen J. Performance evaluation and parametric optimum criteria of an irreversible molten carbonate fuel cell-heat engine hybrid system. Int J Electr Sci 2011;6:4714–29.
[24] Chen L, Zhang H, Gao S, Yan H. Performance optimum analysis of an irreversible molten carbonate fuel cell–Stirling heat engine hybrid system. Energy 2014;64:923–30.
[25] Chen X, Pan Y, Chen J. Performance and evaluation of a fuel cell-thermoelectric generator hybrid system. Fuel Cells 2010;10:1164–70.
[26] Chen X, Chen L, Guo J, Chen J. An available method exploiting the waste heat in a proton exchange membrane fuel cell system. Int J Hydrogen Energy 2011;36:6099–104.
[27] Holman JP. Thermodynamics. 3rd ed. New York: McGraw-Hill; 1980.
[28] Chen J, Lin B, Wang H, Lin G. Optimal design of a multi-couple thermoelectric generator. Semicond Sci Technol 2000;15:184–8.
[29] Zhao Y, Chen J. Modeling and optimization of a typical fuel cell-heat engine hybrid system and its parametric design. J Power Sources 2009;186:96–103.
[30] Chen X, Lin B, Chen J. General performance characteristics and parametric optimum criteria of a Braysson-based fuel cell hybrid system. Energy Fuels 2009;23:6079–84.
[31] Verhaert I, De Paepe M, Mulder G. Thermodynamic model for an alkaline fuel cell. J Power Sources 2009;193:233–40.
[32] Duerr M, Gair S, Cruden A, McDonald J. Dynamic electrochemical model of an alkaline fuel cell stack. J Power Sources 2007;171:1023–32.
[33] Chen L, Sun F, Wu C. Thermoelectric-generator with linear phenomenological heat-transfer law. Appl Energy 2005;81:358–64.